

Plant color adaptation to solar radiation: A study of qualitative and quantitative characteristics

Irina KOLOMIETS¹ 

¹Institute of Ecology and Geography, Chisinau, Republic of Moldova

*Correspondence: ikolomiec71@gmail.com; +373 079 467 405

Keywords: adaptation; corolla color; solar irradiance; spectral composition; position of the maximum

Abstract: This paper investigated latitudinal and seasonal variations in the qualitative characteristics of solar radiation (spectral composition, position of the maximum and short-wave boundary) in the ultraviolet and visible regions. It has been established that, depending on the latitude and season, the peaks $\lambda=415$ nm, $\lambda=480$ nm, $\lambda=500-505$ nm, $\lambda=525-535$ nm, $\lambda=575-590$ nm, $\lambda=610-700$ nm, $\lambda=722.5$ nm, $\lambda=735$ nm, $\lambda=740$ nm, $\lambda=760$ nm and $\lambda=765$ nm may appear. Coloring surfaces variants whose absorption spectrum corresponds to these peaks are considered. It has been suggested that the coloration of the corolla in flowering plants is the result of adaptation to the solar spectrum maximum and may determine convergent seasonal and latitudinal coloration in species of flowering plants.

1. Introduction

The resistance of a species to unfavorable factors largely depends on the adaptive capabilities of the reproductive system, as a guarantor of reproduction of the species in the next generation. One of the organs performing protective function of the reproductive system in higher plants is the corolla. It is generally accepted that the corolla protects the reproductive organs from unfavorable environmental factors and attracts pollinators, therefore the characteristics of the corolla, including color, must have adaptive sense.

It has been found that in many cases the evolution of flower color is determined by the sensory preferences of pollinators (Chittka and Menzel, 1992). Local species diversity may also be important: the percentage of species with blue flowers has been reported to increase as species diversity increases, and the most species-poor communities lack blue flowers (Dyer et al., 2020).

The relationship between corolla color and various abiotic factors was also observed. For example, in *Campanula americana* L. (USA), the color intensity is more strongly determined by latitude than by pollinators: plants from higher latitudes have darker petals (Koski and Galloway, 2018). In southern European populations of *Lysimachia arvensis* L., the distribution of blue and red colors is associated with temperature, precipitation and latitude: blue coloration is more common in warmer and sunnier locations, and blue coloration is also associated with earlier flowering times (Arista et al., 2013). Blue-flowered species have been shown to be sensitive to elevated nitrogen and phosphorus concentrations and to elevated soil acidity, and thus soil quality may influence the composition of local flora in relation to corolla color (Berg et al., 2011; Cecchi et al., 2008).

An attempt to summarize the available data on the influence of abiotic and biotic factors on the color of flowers on the Australian continent showed that both the factors

are important, but the biotic appears to be the main evolutionary factor in corolla color forming in flowering plants (Dalrymple et al., 2020). However, it can be noted that there is still no consensus on the hierarchy of color formation factors.

In this work, we decided to consider another abiotic factor that has not been taken into account until now - latitudinal and seasonal differences in the composition of the solar radiation spectrum. With latitude and season, the average daily height of the sun above the horizon and, consequently, the average amount of air mass through which sunlight passes changes. Since atmospheric absorption differs for different wavelengths, a change in optical mass leads to a shift of the peak of incoming radiation to a different range. We study the latitudinal and seasonal variations in the position of radiation maximum and predict the expected color of absorbing surfaces (corollas of flowering plants), the absorption peak of which coincides with the peak of incoming radiation. We assume that there must be an evolutionary tendency towards the appearance of such surfaces, which, according to our assumption, are maximally adapted. Finally, we check the agreement of our hypothesis with the global statistics data.

2. Materials and Methods

For different latitudes and calendar dates, the solar spectral irradiance was calculated at different wave lengths under conditions of a clear atmosphere. First, for the chosen latitude and date, the average height of the sun above the horizon was calculated, which was taken to be half the noon height, and for the case of a polar day, the average value between the maximum and minimum height. The sun's altitude values were taken from publicly available astronomical tables. For the average height of the sun determined in this way, the value of the air mass AM that attenuates the radiation was calculated using the Bemporad table (Sivtsov, 1968). For the found air mass value, the solar radiation intensity E ($\text{W m}^{-2} \mu\text{m}^{-1}$) was calculated for various wavelengths. For the calculations, we used Table 4 from NASA Technical Memorandum 82021 (Mecherikunnel and Richmond, 1980), compiled for an absolutely clear atmosphere ($\alpha=1.3$, $\beta=0.02$) with water vapor pressure $\text{H}_2\text{O}=20$ mm and ozone $\text{O}_3=3.4$ mm and for different AM values from 1 to 10. E values were calculated by extrapolation between the nearest AM values, and for $\text{AM}>10$ the exponential continuation of the $E(\text{AM})$ function was used.

As a result, for different latitudes with a step of 1° and various calendar dates with a step of 1 month, spectrograms were compiled in the range of 375-765 nm with a step of 5 nm, characterizing the dependence of E on the wavelength λ . For each spectrogram, the position of the peaks λ_{max} , with which local maxima E were associated, was determined. Photon energies for given values of λ were calculated using the Planck equation (Turro, 1967; Kwiat, 2022).

A pigmented surface, the absorption peak of which coincides with λ_{max} , is assumed within the framework of the model under consideration to be maximally adapted to solar radiation of a given latitude and a given season.

Data on the distribution of plant species by corolla color are taken from Kattge et al., 2020, where global statistics cover about 10 000 species.

3. Results

3.1. Qualitative characteristics of solar radiation

The main qualitative characteristics of solar radiation are the spectral composition, the position of the maximum, and the short-wave boundary, which depend on the height of the Sun above the horizon and on the optical mass of the atmosphere (Air Mass - AM) (Tab. 1). It is known that the lower the Sun descends, the richer its spectrum in long-wave radiation, and the short-wave boundary and radiation maximum are shifted towards longer wavelengths. Since at latitude 50° - 60° in the winter months the Sun does not rise above the horizon higher than 6.5° - 16.5° (Table 1), it follows that in winter at

these latitudes in the solar spectrum there is no ultraviolet radiation with wavelengths shorter than 360 nm. In summer, the ultraviolet end of the spectrum extends up to 295 nm (Mecherikunnel and Richmond, 1980; Sivcov, 1968).

Table 1. Latitudinal variation of the Sun height above the horizon ($h,^\circ$) and the daily mean optical mass of the atmosphere (AM) at the solstices and equinoxes

Date	December 22		March 21		June 21		September 23	
Latitude, °	h	AM	h	AM	h	AM	h	AM
90	-	-	0	39.600	23.5	2.500	0	39.600
80	-	-	10	10.400	33.5	2.500	10	10.400
70	-	-	20	5.600	43.5	2.500	20	5.600
60	6.5	14.650	30	3.820	53.5	2.220	30	3.820
50	16.5	6.720	40	2.900	63.5	1.895	40	2.900
40	26.5	4.300	50	2.360	73.5	1.670	50	2.360
30	36.5	3.170	60	2.000	83.5	1.500	60	2.000
20	46.5	2.525	70	1.740	86.5	1.455	70	1.740
10	56.5	2.105	80	1.550	76.5	1.610	80	1.550
0	66.5	1.820	90	1.410	66.5	1.820	90	1.410
-10	76.5	1.610	80	1.550	56.5	2.105	80	1.550
-20	86.5	1.455	70	1.740	46.5	2.525	70	1.740
-30	83.5	1.500	60	2.000	36.5	3.170	60	2.000
-40	73.5	1.670	50	2.360	26.5	4.300	50	2.360
-50	63.5	1.895	40	2.900	16.5	6.720	40	2.900
-60	53.5	2.220	30	3.820	6.5	14.650	30	3.820
-70	43.5	2.500	20	5.600	-	-	20	5.600
-80	33.5	2.500	10	10.400	-	-	10	10.400
-90	23.5	2.500	0	39.600	-	-	0	39.600

Note. The gray cell gradient indicates a decrease in optical mass, "-" - polar night. Latitudes of the southern hemisphere are denoted as negative. AM is an indicator of the atmospheric influence on the intensity of solar radiation reaching the Earth's surface, called the optical mass of the atmosphere.

At the moments of the spring and autumn equinoxes, the height of the Sun above the horizon ($h,^\circ$) and the optical mass of the atmosphere (AM) change symmetrically relative to the equator line (0°). The optical mass decreases in the direction from the north pole to the equator and increases from the equator to the south pole, and the Sun height above the horizon, on the contrary, increases in the direction from the north pole to the equator and decreases from the equator to the south pole. At the winter solstice, the symmetry center shifts to the South Pole by 23° , causing the phenomena of polar night at the North Pole and polar day at the south pole. At the summer solstice, the symmetry center shifts to the north pole by 23° , causing the phenomena of polar night at the south pole and polar day at the north pole. Variation of h and AM depending on the season has a sinusoidal pattern and causes changes in the main qualitative and quantitative characteristics of solar radiation: spectral composition, position of the maximum, short-wave boundary, and intensity (Table 2, Figure 1).

A detailed analysis of the spectral distribution of solar radiation at 5 nm and 1° latitude revealed the presence of the following peaks and their shifts: violet peak ($\lambda=415$ nm, AM=1; $\lambda=420$ nm, AM=1.5; 2), blue peak ($\lambda=480$ nm, AM=1, 1.5, 2, 3, 4), cyan ($\lambda=500$ nm, AM = 1, 1.5, 2, 3; $\lambda=505$ nm, AM=4). The green maximum appears beginning at $\lambda=525$ nm (AM=1, 1.5) and shifts to $\lambda=530$ nm at AM=1.5, 2, 3, and to $\lambda=535$ nm at AM=4. The yellow peak $\lambda=575$ nm is observed at AM=1, and at AM=1.5, 2, 3, 4 it shifts by 15 nm ($\lambda=590$ nm). The red region of the solar spectrum is

represented by the cascade of shifting peaks: $\lambda=610\text{--}700\text{ nm}$ ($AM=2\text{--}10$), $\lambda=722.5\text{ nm}$ and $\lambda=760\text{ nm}$ (at all latitudes, $AM=1\text{--}10$), $\lambda=735\text{ nm}$ and $\lambda=765\text{ nm}$ ($AM=1\text{--}7$), $\lambda=740\text{ nm}$ ($AM=1\text{--}4$).

Table 2. Distribution of solar energy maxima ($E, \text{W m}^{-2} \mu\text{m}^{-1}$) of visible range (λ, nm) at the points of the vernal and autumnal equinoxes

λ, nm	Latitude, °									E, eV
	90	80	70	60	50	40	30	20	10	
375	0	53	235	385	493	566	615	646	662	667
415	0	206	581	822	977	1076	1140	1180	1200	1207
420	0	220	598	834	985	1080	1142	1180	1200	1207
480	0	554	1047	1294	1439	1526	1581	1615	1633	1638
495	0	593	1055	1279	1408	1485	1533	1563	1578	1583
500	0	612	1068	1286	1410	1485	1532	1561	1575	1580
505	0	617	1066	1280	1402	1475	1520	1548	1563	1568
525	1	642	1070	1268	1381	1448	1490	1515	1528	1533
530	1	651	1075	1270	1381	1447	1488	1513	1525	1530
535	1	654	1071	1262	1370	1434	1474	1498	1511	1515
575	3	692	1073	1242	1336	1392	1426	1447	1458	1461
585	3	704	1081	1247	1338	1393	1426	1447	1457	1461
610	6	732	1078	1227	1309	1357	1387	1404	1413	1417
640	16	809	1105	1226	1292	1329	1352	1366	1373	1376
650	23	835	1111	1222	1282	1317	1338	1350	1357	1359
660	28	848	1111	1216	1273	1305	1324	1336	1342	1344
700	65	890	1096	1174	1215	1239	1253	1262	1266	1268
710	71	888	1084	1159	1198	1221	1234	1242	1247	1248
722.5	37	711	913	998	1047	1076	1094	1105	1111	1113
735	65	802	985	1058	1097	1120	1135	1143	1147	1149
740	72	812	989	1059	1096	1118	1132	1140	1144	1145
747.5	98	866	1030	1092	1124	1142	1153	1160	1163	1164
765	111	858	1008	1063	1092	1109	1119	1125	1128	1129

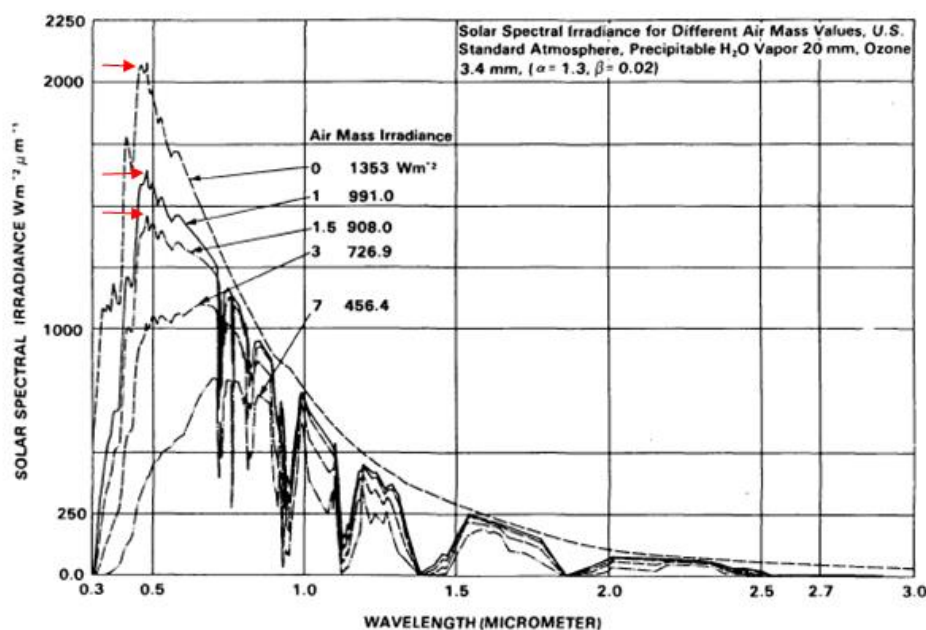


Figure 1. Changes in the intensity, spectral composition, position of the maximum, and shortwave boundary of solar radiation (Mecherikunnel and Richmond, 1980). The red arrows indicate the double maximum in the blue and cyan range.

A latitudinal analysis of the distribution of solar energy maxima during the year showed that in the northern hemisphere, the distribution of radiation maxima is symmetric for the month of June. So, July is symmetric to May, April to August, September is similar to March (points of autumn and spring equinox), October to February, November to January, and December in the southern hemisphere is an axis of symmetry, as well as June in the northern hemisphere (Britton, 1986).

Based on cyclic nature of expression of qualitative characteristics of solar radiation, it is legitimate to assume that the response of biological systems to solar radiation also has a cyclic nature, manifested in the form of adaptations both at latitudinal and seasonal levels. In the process of evolution, biological adaptation of flowering plants may have followed the path of forming light-sensitive surfaces whose absorption maximum coincides with the spectral maximum of incident radiation. The general laws of electromagnetic radiation absorption are fulfilled for such surfaces. They define the relationship between the magnitude of absorption and the amount of the absorbing substance, the pigment. Pigments are characterized by a specific molecular structure, namely, the presence of a system of conjugated double bonds. Depending on the position and number of double bonds, the pigment selectively absorbs electromagnetic radiation. For this reason, each pigment has a corresponding coloring and a specific light absorption curve. The more double bonds in the pigment molecule, the longer its absorption wave. According to the Grotthuss-Draper law (Turro, 1967), only the light which is absorbed by this substance can cause chemical transformation of the substance. It can be tentatively considered that only the light which color is complementary to the visible color of this body, i.e. complements it to white (Table 3) has a chemical effect on a body of a certain color. Using the formulas indicated in Table 3, let us build a model of the corolla, the surface of which was formed as a result of adaptation to the maxima of the solar spectrum. Let us present the formation of the coloration of surfaces optimally adapted to the maxima of solar radiation. The general regularities in the distribution of the solar radiation maxima of the visible range should also be preserved in the distribution of the reflected light maxima of the surfaces adapted to them.

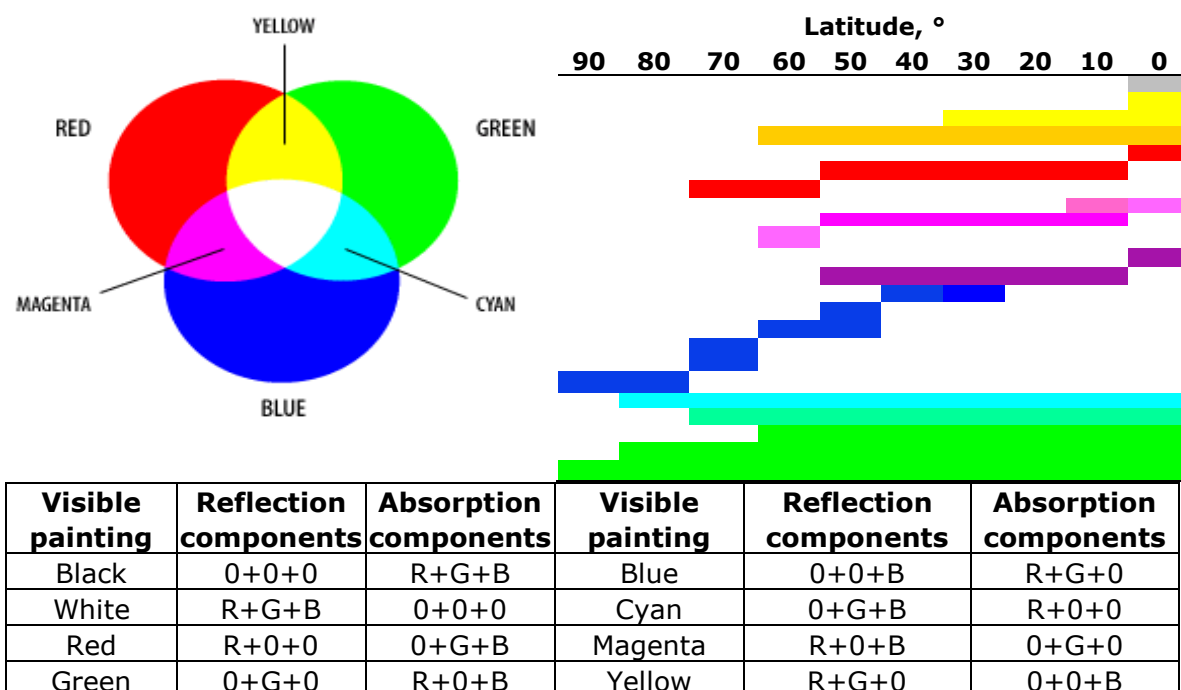
It is obvious that if the radiation and absorption spectrum (Table 2) is ordered in the following direction: uv - violet - blue - cyan - green - yellow - orange - red, then the order of reflection (Table 3) will be as follows: white - yellow - orange - red - magenta - violet - blue - cyan - green, according to RGB color rendering system. The RGB color rendering system is considered to be more efficient in spectral analysis because it corresponds, unlike the RYB color rendering system, to the three types of cones (light sensitive cells to blue, red and green range) in the human retina.

The area of the white maximally adapted surface, as a result of adaptation to the ultraviolet maximum, is at the equator, where AM near noon is close to or equal to one. The area of the yellow adaptive surface (Table 3) is located between 0° and 60° degrees on either side of the light equator (the light equator coincides with the geographic equator at the spring and autumn equinoxes and changes its position during the year following changes in the height of the sun above the horizon.) The red surface area ranges from 0° to 70°, and purple (marginal) surface area ranges from 0 to 60°. The violet area closes within ±50°. The dark blue surface is absent at the equator and begins only after 30° north and south latitude. Note, that absorption maximum corresponding to dark blue surface color have fragmentary and cascade pattern in the 610-710 nm range. Hence, at different latitudes the optimally adapted dark blue surfaces should differ not only in intensity, but also in shade. Dark blue cascades to blue toward the poles.

The light blue (cyan) coloration is characteristic of the 0°-80° latitude. The green surface is characteristic of all latitudes, therefore, in terms of evolution, it is the most adapted to the variation of solar radiation intensity, the shift of the short-wave spectrum boundary, and the position of maxima on the electromagnetic scale (Figure 1). The presented model is characteristic for the points March 21 and September 21. At the summer solstice, the presented pattern shifts by 23° toward the North Pole, and at the winter solstice, it shifts by 23° toward the South Pole. This shift determines the

seasonal specificity of the corolla coloration in flowering plants (Britton, 1986). The long-wave boundary of solar radiation can also cause the appearance of adaptive white surface due to the adaptation to numerous peaks in the IR range (Figure 1).

Table 3. Modeling in RGB coloring system of maximally adapted surfaces at the moments of the vernal and autumnal equinoxes (northern hemisphere)



3.2. Quantitative characteristics of solar radiation

The main quantitative characteristic of solar radiation is the intensity that reaches the earth and varies depending on the time of day, year, location and weather conditions. The intensity of solar radiation in free space at a distance equal to the average distance between the Earth and the Sun is called the solar constant. Its value is 1353 W/m². When passing through the atmosphere, sunlight is attenuated mainly by absorption of infrared radiation by water vapor, ultraviolet radiation by ozone, and scattering of radiation by atmospheric dust particles and aerosols (Fig. 1 shows the spectral distribution of solar radiation intensity under different conditions).

The upper curve (AM0) corresponds to the solar spectrum outside the Earth's atmosphere (for example, on board a spacecraft), i.e., at zero air mass of the atmosphere. It is approximated by the distribution of the radiation intensity of an absolutely black body at a temperature of 5800°K. The AM1 curves illustrate the spectral distribution of solar radiation at the Earth's surface when the Sun is at zenith and 60° above horizon, respectively. The total radiation power is 925 and 691 W/m², respectively (averaging over different weather conditions). The average radiation intensity on the Earth is about the same as the radiation intensity at AM=1.5 (the Sun is at an angle of 45° to the horizon) (Mecherikunnel and Richmond, 1980; Sivcov, 1968). Near the Earth's surface, we can assume an average solar radiation intensity of 635 W/m². On a very clear sunny day, this value ranges from 950 W/m² to 1220 W/m². The average value is about 1000 W/m² or 860 kcal/(m²h). To simplify the calculation on the solar energy inflow, it is usually expressed in hours of sunshine with an intensity of 1000 W/m² (Sivcov, 1968).

The previously defined boundaries of the maximum adapted surfaces were based on finding the position of maximum value of solar radiation intensity in the ultraviolet and visible range, at the selected latitude. If we analyze the value of the solar radiation intensity along the meridian, we can easily notice its increase in the direction from the

poles to the light equator. Thus, the surface maximally adapted to the latitudinal maximum, as it approaches the equator, should increase the concentration of pigment absorbing in this range. If the latitudinal maximum is in the equatorial zone, the pigment concentration should decrease as it moves away from the equator (Table 2). Increasing pigmentation will decrease the albedo of the surface and contribute to its overheating. Therefore, as we approach the equator, the natural selection will be directed toward a surface with high reflectivity, ideally a white surface.

It is logical to assume that in the presence of several peaks; the dominant coloration of the maximally adapted surface would be complimentary to the peak of highest intensity. However, in the presence of peaks displaying in complementary ranges and equal in photon quantity, adaptation should occur to both the ranges simultaneously, which led to reflection in mutually complementary ranges, and, therefore, resulting in a white surface with the highest albedo value. It should be noted that for a model surface the condition is accepted that transparence coefficient is uniform and not equal 0.

For maxima located in northern latitudes, which are characterized by low photon density, maximum adapted are surfaces of green, blue and cyan colors, according to RGB system. In this case the selection should be directed towards increasing the pigment molecules number, to decrease albedo and increase flower temperature as a protective function against cooling. According to Stark-Einstein quantum-optical equivalence law (Turro 1967, Kviat, 2022), each absorbed photon causes photochemical excitation of only one molecule. Therefore, the number of photons of a certain range must be in an equivalent ratio to the number of pigment-trap molecules. Let's calculate the number of photons for flows of 1 μm width.

Let's calculate the photon energy E for each maximum according to Planck equation, and by dividing the flux energy P by the photon energy, we find out the photon flux density n (Turro, 1967; Kviat, 2022):

$$E = \frac{hc}{\lambda} \quad (1)$$

$$n = \frac{P\lambda}{hc} \quad (2)$$

where $h = 6.63 \cdot 10^{-34} \text{ J}\cdot\text{s}$ is Planck's constant, $c = 3 \cdot 10^8 \text{ m/s}$ is the speed of light, λ is the wavelength (1 nm = 10^{-9} m).

Based on the results obtained (Table 4), we can conclude that in terms of photon number the light fluxes of the short-wave range are always less than those of the long-wave range. It follows that the surfaces adapted to the long-wave range prevail over the surfaces adapted to the short-wave range. Calculating photon number ratio of the complementary bands (their equal values give in total white color) shows that at the latitudes where complementary bands ratio is close to 1 (530 nm/740 nm; 10°N and 10°S) the probability of the appearance of maximally adapted surfaces of white color in the course of the evolution is high (Table 5). Thus, the combination of high and uniform absorption capacity of the working surface in complementary bands may be the cause of white-flowering in higher plants.

Table 4. Distribution of photon flux ($10^{19} \text{ m}^{-2} \text{ s}^{-1} \mu\text{m}^{-1}$) by maxima of visible range radiation (λ , nm) at the points of vernal and autumnal equinoxes

E, eV	Latitude, °									
	90	80	70	60	50	40	30	20	10	0
3.3	0	10	44	73	93	108	116	123	126	126
3.0	0	43	121	171	204	224	238	246	250	251
2.95	0	46	126	176	208	228	241	249	253	255
2.6	0	133	252	311	346	367	380	388	393	394
2.5	0	148	264	320	352	371	383	391	394	396
2.48	0	154	269	324	356	374	386	393	397	398

E, eV	Latitude, °									
	90	80	70	60	50	40	30	20	10	0
2.46	0	157	271	325	356	375	386	393	397	398
2.36	0	170	283	336	366	384	394	401	404	406
2.34	0	174	287	339	369	386	398	404	408	409
2.3	0	178	291	343	373	389	401	407	411	412
2.16	1	200	311	359	387	403	413	419	422	423
2.1	1	209	322	371	398	414	424	431	434	435
2.00	2	229	337	384	409	424	434	439	442	443
1.92	5	263	360	399	421	433	440	444	447	448
1.91	8	273	364	400	419	431	438	442	444	445
1.88	9	282	369	404	423	434	440	444	446	447
1.77	23	314	387	414	429	438	443	446	447	448
1.75	26	317	387	414	428	436	441	444	446	446
1.72	14	258	332	363	381	391	398	401	404	404
1.69	24	297	364	391	406	414	420	423	424	425
1.68	27	302	368	394	408	416	421	424	426	426
1.63	38	332	395	419	431	438	442	445	446	446
1.62	43	331	389	410	421	428	432	434	435	436


Table 5. Ratio of photon number in complementary bands of the solar spectrum at the points of vernal and autumnal equinoxes

Complementary ranges λ_1/λ_2	Latitude, °								
	90	80	70	60	50	40	30	20	0
420 nm/585 nm	0.0	0.2	0.5	0.5	0.6	0.6	0.6	0.6	0.6
480 nm/650 nm	0.0	0.5	0.8	0.8	0.9	0.9	0.9	0.9	0.9
500 nm/722.5 nm	0.0	0.6	0.9	0.9	1.0	1.0	1.0	1.0	1.0
530 nm/740 nm	0.0	0.6	0.9	0.9	0.9	0.9	1.0	1.0	1.0

Note: The gray color indicates near equilibrium ration causing the appearance of white-flowering.

It is noteworthy that, in accordance with the model of color formation (Table 3), unequal ratios of complementary ranges can lead to the formation of a surface of mixed color. Since photon flux in each band is different, perhaps it forms the corresponding frequency distribution of the maximum adapted surfaces. Integration of the ultraviolet and visible part of the solar spectrum over the color ranges showed a correspondence between theoretical frequencies of maximally adapted surfaces and empiric global frequencies of species with yellow, red, purple and blue corolla coloration (Table 6). Disagreement for white corolla species is caused by the failure to take into account all variants, for which the ratio between the main and complementary range is close to or equal to 1. Disagreement for green corolla species is caused by non-separability of vegetative leaf coloration from flower petal coloration. It is especially noteworthy that white-flowering generators are blue and green ranges.

Table 6. Theoretically assumed and empirical global frequencies of flower colors (Kattge et al., 2020) based on human visual perception ($N = 10\,437$ species)

Flowe color								
Species number	2466	2103	404	443	2121	772	1559	569
Species number, %	24.0	24.0	4.0	20.0	7.0	15	5	
Theoretically expected frequency, %	4.9	23.7	4.6	19.4	7.3	40.0		

As for the equal-level ratios of complementary ranges by energies, this question requires a detailed study from the point of view of plant organism thermoregulation. As a color-forming index, unequal ratios in photon number are much more interesting, because they form a great variety of corolla color tints, creating coloristic richness of plant species and huge material for natural selection. Using modern electronic programs and the ratios presented, it is possible to predict in which direction the selection will act in a certain area and at a certain time. Which species are preferably planted at any given point on the globe in order to maximize productivity and profit.

It should be noted that the given model of the maximum adapted surface was calculated for a completely clear sky. When the sky is overcast, the distribution pattern of both the solar radiation maxima and the coloring of maximally adapted surfaces shifts toward the large air masses (from the equator to the pole). Accordingly, the seasonal features will also change with latitude shift in the corolla color distribution by 23° at the summer solstice and by -23° at the winter solstice (Figure 2).

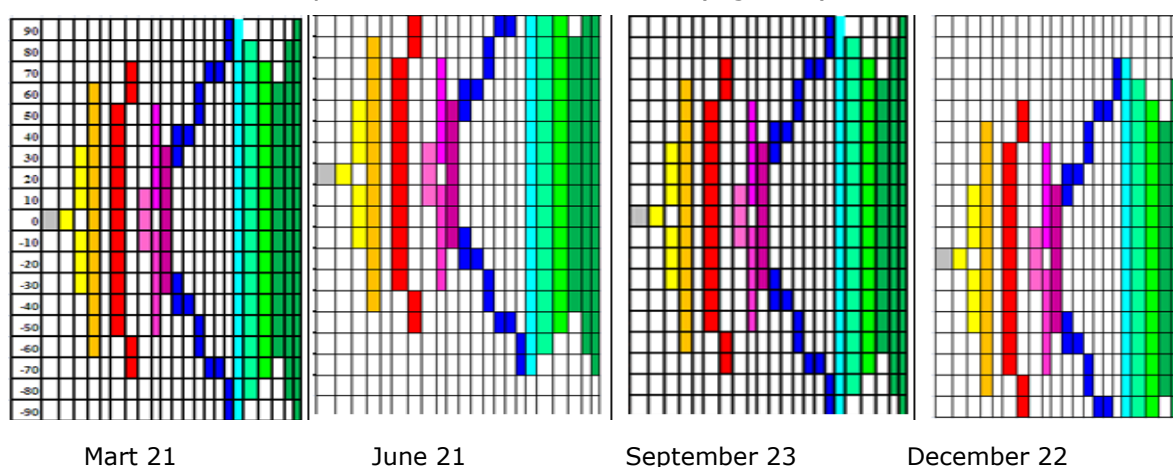


Figure 2. Model of the latitudinal distribution of most adapted surface color in different seasons

4. Discussion

The search for patterns that determine the diversity of plant systems and plant communities is a serious problem in plant ecology. Establishing such patterns can provide an answer to the causes of species extinction and help in the search for methods of restoration and conservation of species richness. By some authors, geographical patterns (Kolomiets, 2021) of petal color in flowering plants were explained by the temperature characteristics of species habitat (Lacey et al., 2010), acidity (Stavenga et al., 2021) and nutritional qualities of the soil, distance to the glacial refugium (Koski and Galloway, 2018).

All the above factors are combined in our model of adaptation of flowering plants to solar spectrum maxima. A change in the position of the maximum of the solar spectrum is the cause of variation in temperature, humidity and other abiotic and biotic factors. The results obtained on adaptation to the near red range maxima ($\lambda=610-710$ nm) at $30-90^\circ$ N and S latitude explains the paucity of blue corolla species, their absence at the equator and presence at the Mediterranean, and their appearance at 50-es latitudes at the point of summer and winter solstice.

The presented model of maximally adapted surfaces well explains the phenomenon of intra-specific color polymorphism, as well as the appearance of various shades of basic colors, as an adaptation to different photon densities in the same range. This assumption will allow us to look at the domestic species origin centers in terms of the geographical conditionality of their polymorphism.

5. Conclusions

- 1) Most of the globe's surface is, according to the RGB system, exposed to two main types of radiation: extended blue (violet, dark blue and light blue) and red (near-red and far-red). The green-yellow maximum is transitional between two main types of solar radiation maxima.
- 2) Detailed analysis of the spectral distribution of solar radiation at 5 nm and 1° latitude revealed the following peaks and their shifts: purple ($\lambda=415$ nm, AM=1; $\lambda=420$ nm, AM=1.5; 2), blue ($\lambda=480$ nm, AM=1, 1.5, 2, 3, 4) and cyan ($\lambda=500$ nm, AM = 1, 1.5, 2, 3; $\lambda=505$ nm, AM = 4). The green peak appears beginning at $\lambda=525$ nm (AM=1, 1.5) and shifts to $\lambda=530$ nm at AM=1.5, 2,3 and to $\lambda=535$ nm at AM=4. The yellow peak $\lambda=575$ nm is observed at AM=1; at AM=1.5, 2, 3, 4 it shifts by 15 nm ($\lambda=590$ nm). The red range of the solar spectrum is represented by numerous peaks: the shifting peak $\lambda=610-700$ nm (AM=2-10), peaks $\lambda=722.5$ nm and $\lambda=760$ nm expressed at all latitudes (AM=1-10), peaks $\lambda=735$ nm and $\lambda=765$ nm (AM=1-7) and peak $\lambda=740$ nm (AM=1-4).
- 3) The maximum adapted to solar radiation penetrating through the atmosphere would be a surface with absorption maxima in the two main ranges, blue and red (like chlorophyll).
- 4) The radiation-absorption spectrum is ordered in the following direction: violet - blue - cyan - green - yellow - orange - red. According to the RGB color rendering system, the reflection order will be as follows: white - yellow - orange - red - purple - violet - blue - cyan - green.
- 5) The percentage distribution of frequencies in a random sample of 10 437 plants for yellow, red, purple, and blue corolla coloration corresponds to the percentage distribution of the integral energies of the solar spectrum in the corresponding ranges. Thus, the spectral width of the ranges of the visible solar spectrum, is in an associative relationship with the frequency of corolla color in a randomized sample of flowering plants.
- 6) The adaptive potential of the maximum adapted surface increases in the following direction: red (4.6%) < white (4.9%) < blue (7.3%) < purple (19.4%) < yellow (23.7) < green (40%).
- 7) The fragmentary pattern of blue-species distribution is caused by fragmentary distribution of the red-range maxima.

Acknowledgments: The author is deeply grateful to dr. Vorontsov V.A. and dr. hab. Mikhailov M.E. for their help in editing the article.

Funding: Research was carried out within the project of the State Program 20.80009.707.11 "Assessing the sustainability of urban and rural ecosystems to ensure their sustainable development", financed by the National Agency for Research and Development of the Republic of the Republic of Moldova.

References

1. Arista, M.; Talavera, M.; Berjano, R.; Ortiz, P.L. (2013) Abiotic factors may explain the geographical distribution of flower color morphs and the maintenance of color polymorphism in the scarlet pimpernel. *J Ecol*, 101(6), 1613-1622. <https://doi.org/10.1111/1365-2745.12151>
2. Berg, L.G.L. van den; Vergeer, P.; Rich, T.C.G.; Smart, S.M.; Guest, D.; Ashmore, M.R. (2011) Direct and indirect effects of nitrogen deposition on species composition change in calcareous grasslands. *Global Change Biology*, 17(5), 1871-1883. <https://doi.org/10.1111/j.1365-2486.2010.02345.x>
3. Britton, G. (1986) Biochemistry of natural pigments; Cambridge University Press, 1986; 422 p.

4. Cecchi, M.; Dumat, C.; Alric, A.; Felix-Faure, B.; Pradere, P.; Guiresse, M. (2008) Multi-metal contamination of a calcic cambisol by fallout from a lead-recycling plant. *Geoderma*, 144(1), 287-298. <https://doi.org/10.1016/j.geoderma.2007.11.023>
5. Chittka, L.; Menzel, R. (1992) The evolutionary adaptation of flower colours and the insect pollinators' colour vision. *J Comp Physiol A*, 171, 171-181. <https://doi.org/10.1007/BF00188925>
6. Dalrymple, R.L.; Kemp, D.J.; Flores-Moreno, H.; Laffan, S.W.; White, T.E.; Hemmings, F.A.; Moles, A.T. (2020) Macroecological patterns in flower color are shaped by both biotic and abiotic factors. *New Phytologist*, 228(6), 1972-1985. <https://doi.org/10.1111/nph.16737>
7. Dyer, A.G.; Jentsch, A.; Burd, M.; Garcia, J.E.; Giejsztowt, J.; Camargo, M.G.G.; Tjörve, E.; Tjörve, K.M.C.; White, P.; Shrestha, M. (2021) Fragmentary blue: resolving the rarity paradox in flower colors. *Front Plant Sci*, 11, 618203. <https://doi.org/10.3389/fpls.2020.618203>
8. Kattge, J.; Bönsch, G.; Díaz, S.; Lavorel, S.; Prentice, I.C.; Leadley, P.; et al. (2020) TRY plant trait database-enhanced coverage and open access. *Glob Chang Biol*, 26(1), 119 -188. <https://doi.org/10.1111/qcb.14904>
9. Kolomiets, I. (2021) Spatio-temporal variation in the composition of the solar spectrum and its possible evolution. *ECOTERRA - Journal of Environmental Research and Protection*, 18(2), 1-9. https://www.researchgate.net/publication/376687389_Spatio-temporal_variation_in_the_composition_of_the_solar_spectrum_and_its_possible_evolution
10. Koski, M.H.; Galloway, L.F. (2018) Geographic variation in pollen color is associated with temperature stress. *New Phytologist*, 218(1), 370-379. <https://doi.org/10.1111/nph.14961>
11. Kviat, D. (2022) Planck's constant - the result of connecting two strings. *Journal of High Energy Physics, Gravity and Cosmology*, 8(4), 919-926. <https://doi.org/10.4236/jhepgc.2022.84062>
12. Lacey, E.; Lovin, M.; Richter, S.; Herington, D. (2010) Floral Reflectance. Color and Thermoregulation: What Really Explains Geographic Variation in Thermal Acclimation Ability of Ectotherms? *Journal of The American Naturalist*, 175 (3), 335-349. <https://doi.org/10.1086/650442>
13. Mecherikunnel, A.T.; Richmond, J.C. (1980) *Spectral Distribution of Solar Radiation*. NASA-TM-82021; 41 p. Available online: <https://ntrs.nasa.gov/api/citations/19810016493/downloads/19810016493.pdf>
14. Sivcov, S.I. (1968) *Methods for calculating the characteristics of solar radiation*. Hydrometeorological Publishing House "Leningrad": Rusia, 1968; 234 p.
15. Stavenga, D.G.; Leertouwer, H.L.; Dudek, B.; van der Kooi, C.J. (2021) Coloration of flowers by flavonoids and consequences of pH dependent absorption. *Front Plant Sci*, 11, 600124. <https://doi.org/10.3389/fpls.2020.600124>
16. Turro, N. (1967) *Molecular photochemistry*; New York, 1967; 483 p.
17. Warren, J.; Mackenzie, S. (2001) Why are all color combinations not equally represented as flower-colour polymorphisms? *New Phytologist*, 151(1), 237-241. <https://doi.org/10.1046/j.1469-8137.2001.00159.x>

